Dynamic Light Scattering and Fluorescence Study of the Interaction between Double-Stranded DNA and Poly(amido amine) Dendrimers

Marie-Louise Örberg,* Karin Schillén, and Tommy Nylander

Physical Chemistry 1, Center for Chemistry and Chemical Engineering, Lund University, P.O. Box 124, SE-221 00 Lund, Sweden

Received December 18, 2006; Revised Manuscript Received February 20, 2007

The interaction between a cationic poly(amido amine) (PAMAM) dendrimer of generation 4 and double-stranded salmon sperm DNA in 10 mM NaBr solution has been investigated using dynamic light scattering (DLS) and steady-state fluorescence spectroscopy. The structural parameters of the formed aggregates as well as the complex formation process were studied in dilute solutions. When DNA is mixed with PAMAM dendrimers, it undergoes a transition from a semiflexible coil to a more compact conformation due to the electrostatic interaction present between the cationic dendrimer and the anionic polyelectrolyte. The DLS results reveal that one salmon sperm DNA molecule forms a discrete aggregate in dilute solution with several PAMAM dendrimers with a mean apparent hydrodynamic radius of 50 nm. These discrete complexes coexist with free DNA at low molar ratios of dendrimer to DNA, which shows that cooperativity is present in the complex formation. The formation of the complexes was confirmed by agarose gel electrophoresis measurements. DNA in the complexes was also found to be significantly more protected against DNase catalyzed digestion compared to free DNA. The number of dendrimers per DNA chain in the complexes was found to be approximately 35 as determined by steady-state fluorescence spectroscopy.

Introduction

Deoxyribonucleic acid (DNA) is the carrier of genetic information. It is a highly charged anionic polyelectrolyte with an effective density of one negative charge per 0.17 nm and a persistence length of about 50 nm. In recent years, DNA condensation using different cationic specimen has been studied extensively as a way of replacing viral vectors as gene carriers for in vivo gene transfer. Surfactants like CTAB or DODAB, histones, as well as synthetic polymers like poly(amido amine) (PAMAM) dendrimers, polylysine, or poly(ethylene imine) (PEI) are a few examples of those specimens used.[1−6]

In the present work, PAMAM dendrimers of generation 4 (G4) containing 64 surface groups composed of primary amines have been used as the vehicle for compaction of linear salmon sperm DNA (2000 base pairs). The complex formation process has been extensively studied using dynamic light scattering and steady-state fluorescence spectroscopy at different mixing ratios. A PAMAM dendrimer is a radially branched polymer containing amido amine groups emanating from a central ethylenediamine core. Dendrimers have a supramolecular structure with an exact composition and constitution. However, the conformation depends on the number of generations, and flexible dendrimers of fourth generation have been found to show a fluctuating structure. The structure is also very sensitive to the ionic strength where a more extended structure is formed at low amounts of salt due to the intramolecular interaction. The radial structure of dendrimers has been investigated, and dendrimers of fourth generation have been shown to be soft and flexible containing a dense core.[7−9] Although the interaction between PAMAM dendrimers and DNA in aqueous medium has been studied extensively, the complex formation process in the dilute regime is still not fully understood. Few structural investigations using linear DNA have been performed, and the discrete aggregates containing one DNA molecule have not been characterized in detail. The degree of in vitro transcription and translation when varying the amount of dendrimers present has been studied, but not been clearly related to the structure of the DNA−dendrimer aggregates.[10−16] Dynamic light scattering (DLS) is a useful tool to explore the size and structure of the aggregates formed, with which also the effect of DNA lengths and dendrimer sizes on the complex formation process can be revealed. Previously, DLS has been used to study the interaction of short, 150 bp, DNA molecules with hyper-branched PEI for which the contour length of the DNA is less than the persistence length.[17]

The long-term objective of this work is to design a module for DNA packaging, where the packing and thereby the transcription can be switched on and off. This module would be a transcription competent synthetic analogue of a real cell nucleus.

Experimental Section

Materials. Salmon sperm DNA of 2000 ± 500 bp was purchased from Invitrogen and used as received. Sodium bromide, NaBr (purity 99%), bought from Aldrich was used without any further purification. Poly(amido amine) (PAMAM) dendrimers of generation 4, each with the external surface covered by 64 primary amine groups, were purchased from Sigma and dialyzed against 10 mM NaBr in water prior to use. The purity and polydispersity of the dendrimers were not checked.

DNA, NaBr, and PAMAM dendrimer stock solutions were prepared in 10 mM NaBr solution that was prefiltered using 0.2 μm Minisart filter (Sartorius, Germany). The DNA concentration was measured spectrophotometrically at λ= 260 nm using an extinction coefficient

* To whom correspondence should be addressed. E-mail: marie-louise.orberg@fkem1.lu.se.

10.1021/bm061194z CCC: $37.00
Published on Web 04/26/2007

of 20 μg mL^{-1} for double-stranded DNA. The ratio between the absorbance at 260 nm and at 280 nm was checked to be at least 1.8, and the absorbance at 320 nm was negligible, indicating that no significant protein contamination was present. Stock solutions of both DNA and PAMAM dendrimers were stored at 4 °C. The mixtures were prepared by adding an equal amount of the dendrimer solution into an equal amount of the DNA solution. The DNA concentration in the mixtures was fixed at 0.15 mg mL^{-1}, and the dendrimer concentration was varied. Samples were prepared by equilibrating dendrimers with the DNA in polypropylene containers on mixing boards at 25 °C for at least 3 h and not longer than 24 h. Dendrimer−DNA complexation was tested both before and after dendrimer dialysis. The solutions always showed pH values around 7. In this pH range, it can be expected that the primary amine groups on the PAMAM dendrimer are protonated, the pK_a values of which range from 7 to 9.5.[18−20]

Dynamic Light Scattering. The DLS measurements were performed using a ALV/DLS/SLS-5000F, a CGF-8F based compact goniometer system from ALV-GmbH, Langen, Germany. The light source is a diode-pumped Nd:YAG solid-state Compass-DPSS laser operating at 532 nm from COHERENT, Inc., Santa Clara, CA. The scattering cell is immersed in a refractive index matching bath filled with decaline. The temperature of the cell housing was set to 25 ± 0.01 °C. Two multiple τ digital correlators with 320 spaced channels are used. More instrumental details are available elsewhere.[21]

When performing DLS experiments, the intensity fluctuations measured are used to produce the time correlation function $G^{(2)}(t)$. The Siegert relation expresses the relation between the normalized time correlation function of the scattered intensity $g^{(2)}(t)$ and the normalized time correlation function of the electric field $g^{(1)}(t)$:

$$g^{(2)}(t) - 1 = \beta|g^{(t)}(t)|^2 \tag{1}$$

where t is the lagtime and β (≤ 1) is a coherence factor accounting for deviations from ideal correlation and the experimental geometry.

For polydisperse particle sizes, $g^{(1)}(t)$ is given by a Laplace transform:

$$g^{(1)}(t) = \int_0^\infty \tau A(\tau) \exp(-t/\tau) d \ln \tau \tag{2}$$

where τ is the relaxation time and $A(\tau)$ is the relaxation time distribution.

Performing regularized inverse Laplace transformation using the calculation algorithm REPES included in the GENDIST analysis package provides the relaxation time distribution from the intensity correlation function.[21] The REPES algorithm minimizes the sum of the squared differences between the experimental and calculated $g^{(2)}(t)$ and uses a regularization term, adjustable through the probability to reject that in these measurements is set to 0.5. From the data analysis, the relaxation rate ($\Gamma = \tau^{-1}$) is obtained, which is used to calculate the collective diffusion coefficient D.

Fluorescence Spectroscopy. Steady-state fluorescence emission and excitation spectra were recorded using a Perkin-Elmer LS-50B spectrometer. The temperature was controlled by a heating circulator and set to 25 °C. A 10 × 10 mm quartz cuvette from Hellma was used. The DNA binding dye used was Gelstar (Cambrex), which has an excitation maximum (λ_{ex}) of 493 nm and an emission maximum (λ) of 527 nm. Gelstar is known to be highly sensitive for detecting nucleic acids and shows a large fluorescent enhancement upon DNA binding and low/negligible background fluorescence in the absence of DNA. Excitation and emission slits were chosen to be 2.5 nm, and the scanning rate was set to 50 nm min^{-1}. The emission and excitation spectra were recorded between 400 and 700 nm and 200−520 nm, respectively. Two spectra were in all cases accumulated and averaged for each sample in order to ensure good reproducibility. Stock solutions of the nucleic acid stain were prepared by diluting 5 μL of concentrated solution to a total volume of 5 mL in 10 mM NaBr and was stored in polypropylene containers at 4 °C protected from light. Blank spectra were recorded with buffer and dye in the cuvette and were subtracted from all fluorescent signals. Sample volumes of 2 mL were used, where 500 μL of the Gelstar stock solution was added 10 min before measurements to an already diluted sample from the DLS measurements. A final DNA concentration of 2 μg mL^{-1} was used in the fluorescence cuvette.

Gel Electrophoresis. In order to further investigate the structure of the aggregates formed, agarose gel electrophoresis was performed at 90 V and 45 mA for 90 min using TBE as running buffer and agarose from Seakem. Agarose gels of 1%, prestained using Gelstar, were used. Samples prepared for DLS and equilibrated as described previously were diluted to give a final DNA concentration of 48 μg mL^{-1} to be added to each well. A total of 2 μL of orange loading dye solution (Fermentas) was added to each sample, and the total volume injected into each well was 10 μL. In addition, the samples were treated with Turbo DNase (Ambion) to elucidate the relation between the degree of compaction and accessibility since DNase digests DNA. The amount of Turbo DNase added to each mixture was 0.5 μL which is equal to 2 units and enough to degrade 1 μg of free DNA in 5 min at 37 °C. Samples containing DNase were incubated for 15 min at 37 °C in order to ensure full digestion of the accessible parts of the DNA molecules before loading them onto the gels. A ladder (MassRuler) from Fermentas was added to the gels for reference. When the electrophoresis measurements were completed, the DNA in the gels was detected using a Dark Reader (Clare chemicals) where the different bands were visualized.

Results and Discussion

1. Dynamic Light Scattering

1.1 Pure PAMAM Dendrimer and Salmon Sperm DNA Solutions. The pure DNA and pure dendrimer solutions with 10 mM NaBr were studied by using DLS at different concentrations and at scattering angles ranging from 50° to 130°. The apparent translational diffusion coefficient (D) of each macromolecule was determined at finite concentrations in the limit of low scattering vectors from the relaxation rate, Γ, according to:

$$D = \left(\frac{\Gamma}{q^2}\right) \tag{3}$$

where q is the magnitude of the scattering vector expressed as $q = (4\pi n/\lambda)\sin(\theta/2)$, where n is the refractive index of water, λ is the incident wavelength, and θ is the scattering angle.

The Stokes−Einstein relationship is used to relate the diffusion coefficient to the hydrodynamic radius, R_H, of the object that undergoes translational motion:

$$R_H = \frac{kT}{6\pi\eta_0 D_0} \tag{4}$$

where k is the Boltzmann constant and T is the temperature in K. The diffusion coefficient D_0 is obtained from the extrapolation of D to infinite dilution.

A PAMAM dendrimer solution of 18 mg mL^{-1} was characterized by measuring the intensity correlation functions at different angles. Figure 1a presents a typical relaxation time distribution obtained from the inverse Laplace transformation of the correlation function measured at 90°. The linear correlation in the q^2 dependence of Γ, as expected for translational diffusion, is excellent and indicates that $R_{H,app}$ can be determined at 90°. For free PAMAM dendrimers of different concentrations, D was then determined from DLS measurements at $\theta = 90°$. In Figure 1b, the diffusion coefficient corresponding to the diffusive mode is plotted as a function of the dendrimer concentration. The diffusion coefficient is slightly concentration dependent, and extrapolation to infinite dilution gave $D_0 = 9.93 \times 10^{-11}$ m^2 s^{-1}. The hydrodynamic radius of the dendrimer is

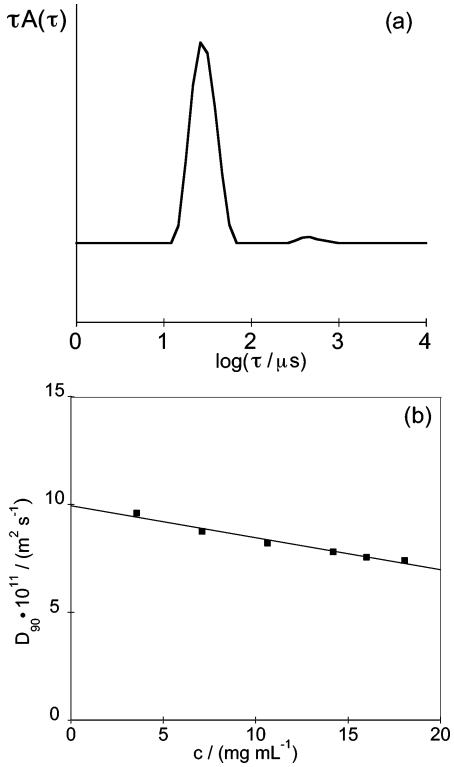

Figure 1. DLS data for free dendrimers in aqueous solution. (a) Relaxation time distribution obtained from REPES analysis at $\theta = 90°$ for a solution of 18 mg mL^{-1} of PAMAM dendrimer in 10 mM NaBr. (b) The apparent diffusion coefficient at $\theta = 90°$ as a function of PAMAM dendrimer concentration.

calculated using the Stokes−Einstein relationship (eq 4) and found to be $R_{H,app} = 24.5$ Å. This is in close agreement with data stated by the manufacturer claiming a diameter of 45 Å. It should be noted that the relaxation time distributions recorded at lower q values ($\theta \approx 65°$ and lower) show an additional low-amplitude mode at longer τ. This suggests a tendency for the dendrimers to aggregate, which previously has been shown for hyperbranched PEI.[17] The relaxation time distribution is an intensity distribution and not a number distribution, which means that even a very small number of large aggregates will give rise to a peak. This may also explain the negative slope in Figure 1b. In line with our study, no significant interdendrimer interaction has been found in dialyzed dendrimer aqueous solutions.[22]

The salmon sperm DNA solution of concentration 0.15 mg mL^{-1} shows two relaxation modes in the relaxation time distribution. The first one is the translational diffusion and the second faster one, here denoted as the internal mode, is a result of internal motions of the coil, which has been discussed in previous literature, see Figure 2a.[23−26] The value of $R_{H,app} = 107 \pm 5$ nm has previously been determined for the salmon sperm DNA molecules in 10 mM NaBr at 25 °C from the diffusion coefficient at infinite dilution being $D_0 = (2.3 \pm 0.1) \times 10^{-12}$ m^2 s^{-1}.[26]

1.2 Dendrimer−DNA Complex Formation. DLS data was obtained from mixed solutions containing 0.15 mg mL^{-1} salmon sperm DNA and a varying amount of dendrimers expressed as the molar ratio $r_{molar} = n_{dendrimer}/n_{DNA}$. Figure 2a shows the relaxation time distributions at 90°. The internal mode can be seen to decrease in amplitude, and the translational diffusion is shifted to faster relaxation times upon increased amount of dendrimers added. An increased diffusion coefficient value in the presence of dendrimers is related to a decreased hydrodynamic radius according to the Stokes−Einstein relationship (eq 4), in agreement with a compaction of the DNA molecule in the presence of cationic PAMAM dendrimers. Salmon sperm DNA has a contour length that is at least 14 times larger than its persistence length; that is, it should behave like a semiflexible chain. The disappearance of the DNA internal mode can therefore be related to the formation of a more compact globule since a homogeneous hard sphere does not express any internal motions.[26] The aggregate size obtained from DLS measurements is constant over a wide range of added amount of dendrimers and a mean value of 50 nm can be calculated, Figure 2b. The aggregation behavior indicates a cooperative complex formation

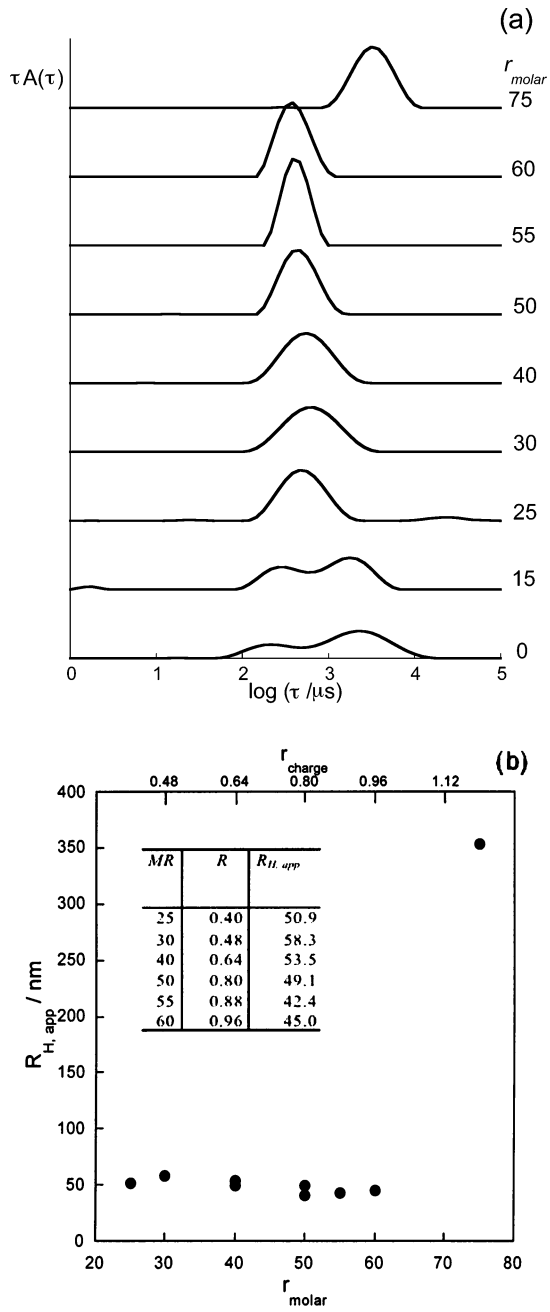

MR	*R*	$R_{H, app}$
25	0.40	50.9
30	0.48	58.3
40	0.64	53.5
50	0.80	49.1
55	0.88	42.4
60	0.96	45.0

Figure 2. DLS data for mixtures of dendrimer and DNA in aqueous solution at 24 h after mixing. (a) Selected relaxation time distributions from DLS measurements at $\theta = 90°$ on 0.15 mg mL^{-1} salmon sperm DNA in 10 mM NaBr with different r_{molar} of PAMAM dendrimers. Also included are the free DNA solution with $r_{molar} = 0$. (b) The hydrodynamic radius of the dendrimer/DNA complex as a function of r_{molar} and r_{charge}. Inset gives the exact values for the hydrodynamic radii measured with DLS.

in dilute solutions. This has previously been suggested to take place between PEI and short DNA fragments as well as for the interaction between cationic surfactants and DNA.[17,27−29] It is evident from our results that the relaxation time distributions for the complexes become narrower when the amount of dendrimers is increased up to $r_{molar} = 60$. At higher r_{molar}, larger aggregates as visualized by the shift of the peak to higher τ at $r_{molar} = 75$. The charge ratio r_{charge} is defined as the ratio between the charged groups on the dendrimer surface, i.e., the primary amines, and the DNA base pairs ($[NH_3^+]/[PO_4^-]$). In our study $r_{molar} = 60$ corresponds to $r_{charge} = 0.96$, which is close to charge neutrality, and the results are interpreted assuming that all DNA interact with dendrimers. It should be noted that, for the calculation of r_{charge}, all primary amine groups of the dendrimers are assumed to be protonated in the conditions used. However, the amount of dendrimers in one aggregate cannot be easily elucidated since all dendrimers will not necessarily be interacting with the DNA. The interaction between two oppositely charged polyelectrolytes like the PAMAM dendrimer and the DNA molecules gives with time rise to associative phase separations at charge ratios above 1. A ratio of 75 dendrimers/DNA, which is equal to $r_{charge} = 1.2$, i.e., just above the calculated point of charge neutrality, gives an increased size of the aggregates formed when measured after 24 h. The increase in the aggregate size can be explained by the formation of aggregates where one dendrimer is in contact with more than one DNA molecule.[27] At a ratio of 100 dendrimers/DNA, a fast associative phase separation is reached resulting in a dilute upper phase and a dense lower phase, both containing dendrimers and DNA. No DLS measurements were performed in this two-phase regime. It should be noted that the increased aggregate size at charge ratios above 1 clearly support the assumption that all primary amines are protonated at the conditions used, experimental values in agreement with calculated values. It should also be noted that further addition to reach a high excess of dendrimers would redissolve the larger aggregates formed in the phase-separated samples. Instead, discrete aggregates of 50 nm observed at lower dendrimer/DNA ratio appear in addition to the slow mode corresponding to large aggregates and the small faster mode corresponding to free dendrimers (data not shown).

2. Fluorescence Spectroscopy

In order to quantify the amount of free DNA at different ratios of dendrimer/DNA, and thereby the composition of the aggregates, steady-state fluorescence spectroscopy was performed using the nucleic acid stain Gelstar (Cambrex). This is based on the fact that DNA in its condensed form is unable to bind to the dye, which gives a fluorescence emission intensity at $\lambda =$ 527 nm (I_{max}) lower than for the corresponding concentration of free DNA without the compacting agent. The emission spectra with the excitation wavelength of $\lambda_{ex} = 493$ nm, recorded for different ratios of dendrimers/DNA, are shown in Figure 3a with the upper curve being free DNA. The fluorescence emission intensity gradually decreases with increased amount of dendrimers present, which indicates that the amount of free DNA decreases with the dendrimer concentration. The dendrimer binding to DNA was concluded to be sufficiently strong to not be displaced by the fluorophore molecules, in agreement with a previous study using Ethidium bromide.[27] The blue shift detected for increasing amount of dendrimers in the samples is most likely a consequence of the change in the environment polarity that the probe is feeling. The excitation spectra, data not shown, were found to be a mirror image of the emission spectra when recorded at $\lambda = 527$ nm for different dendrimer concentrations. In Figure 3b, the correlation between the

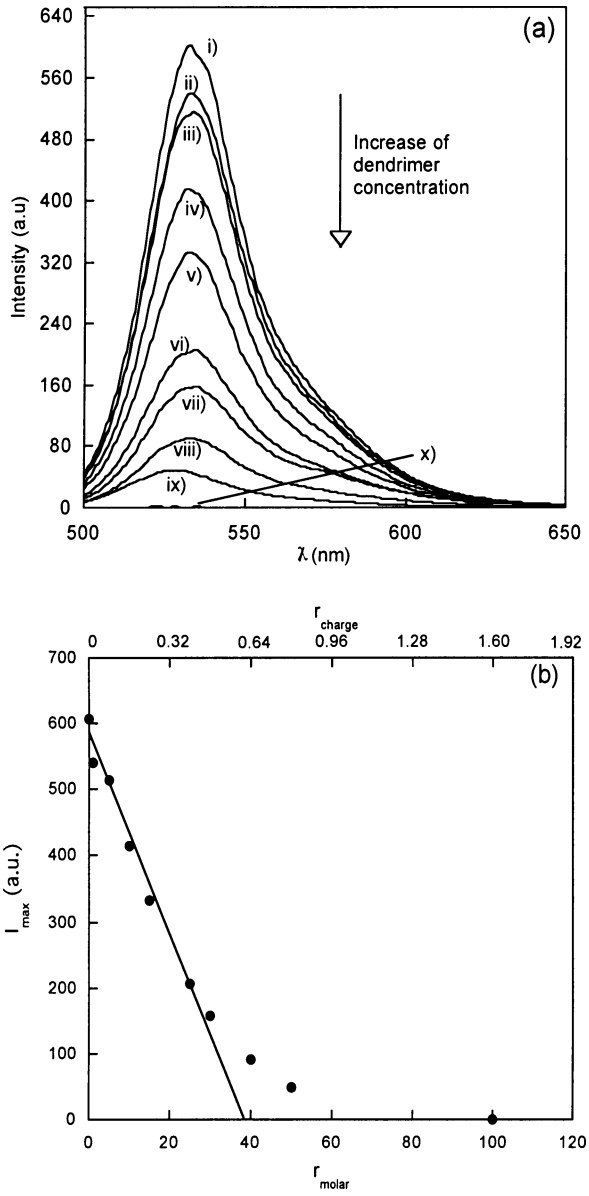

Figure 3. Steady-state fluorescence spectroscopy of dendrimer/DNA containing samples in aqueous solution. (a) Emission spectra for different r_{molar}. The amount of dendrimers increases as indicated. See Table 1 for the definition of the curves marked as i−x. (b) I_{max} as a function of the r_{molar} and r_{charge}.

fluorescence intensity, I_{max}, and the ratio of dendrimer/DNA in the different samples, is shown. The linear fitting included in the plot shows a good agreement with the experimental data for the lower ratios investigated. At 40 dendrimers/DNA, the linear correlation between intensity and concentration is no longer true. The recorded intensity, I_{max}, for all the samples was evaluated using the fact that free DNA solutions of different concentrations without dendrimers show a linear correlation in fluorescence intensity. This is illustrated in Figure 4 where the data points correspond to mean values of two independent measurements of the same DNA concentration. The amounts of free DNA in its native conformation in each sample containing dendrimers is calculated from fluorescence data, see Table 1. The amount of DNA unavailable for the fluorophore to bind to is assumed to be aggregated and was established by subtracting I_{max} for free DNA with the I_{max} for a specific mixture. For the ratio of 100 dendrimers/DNA, the aggregates formed are no longer discrete, explaining the zero intensity measured.

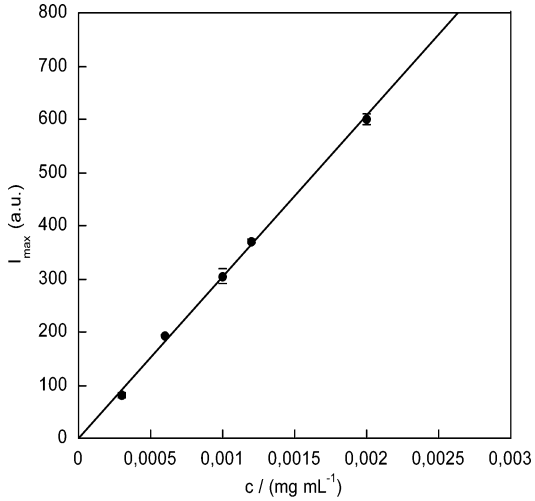

Figure 4. Fluorescence intensity maximum of Gelstar at $\lambda = 527$ nm (I_{max}) for DNA solutions of different concentration.

Table 1. Fluorescence Spectroscopy Emission Data Showing I_{max}, the Amount of Free DNA in Each Sample, as Well as the Calculated Composition of the Discrete Aggregates for the Different Ratios of Dendrimer/DNA Investigated

sample	r_{molar}	r_{charge}	I_{max} (a.u.)	free DNA (μg mL^{-1})	dendrimers per complex
i	–	–	606	2.0 (100%)	–
ii	1	0.016	540	1.8 (90%)	10
iii	5	0.08	515	1.7 (85%)	33
iv	10	0.16	415	1.4 (70%)	33
v	15	0.24	332	1.1 (55%)	33
vi	25	0.4	206	0.68 (34%)	38
vii	30	0.48	158	0.52 (26%)	40
viii	40	0.64	90.5	0.30 (15%)	47
ix	50	0.8	47.9	0.16 (8%)	54
x	100	1.6	0.0	0	–

The number of dendrimers added to a mixture is known and assuming that all dendrimers interact with DNA makes it possible to calculate the composition of one discrete aggregate. A fixed value of 33 dendrimers per complex for the molar ratios of 5, 10, and 15 is obtained. Further addition of dendrimers shows an increased amount of dendrimers present within one discrete aggregate. It is also evident in Figure 3b that the emission intensity for the ratio of 40 dendrimers/DNA is off and that the calculated composition of the discrete aggregates shown in Table 1 should be decreased for a linear correlation to be true. This indicates that at the ratio of 40 dendrimers/DNA, the aggregates start to increase in size. Important to remember is that a few larger aggregates are enough to shift the composition values toward higher ones.

From the fluorescence spectroscopy results we may conclude that below charge neutrality, discrete aggregates containing one DNA molecule are formed with roughly 35 dendrimers. The number of dendrimers calculated to be within one discrete aggregate at higher ratios can be explained by the formation of larger aggregates or dendrimer−dendrimer aggregation.

Important to note is that when the DNA is compacted in the presence of dye, the fluorescence intensity will not decrease to the same extent as the stain is more efficient in remaining bound to DNA when DNA is associated with the dendrimer than to bind to an already condensed molecule. The effect on the fluorescence intensity was also compared with DNA complexed with the cationic surfactant CTAB (data not shown). The intensity was found to gradually decrease in the same way as for dendrimer−DNA mixtures. Cationic surfactants like CTAB are known to bind and condense DNA in a cooperative way. This result supports the theory that dendrimers interact with DNA in the same manner.[28−32]

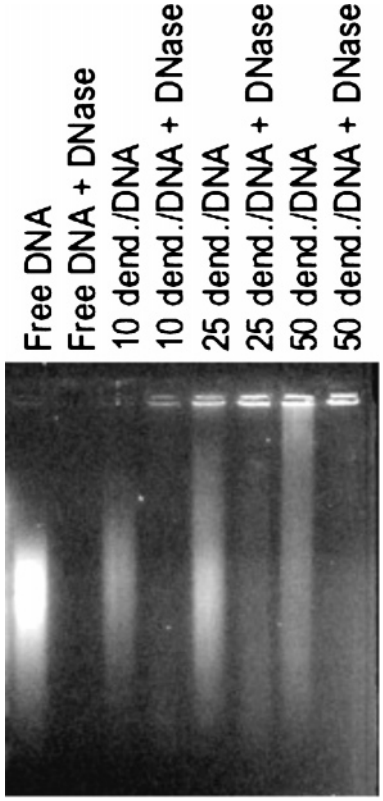

Figure 5. Gel electrophoresis of dendrimer/DNA complexes of varying dendrimer concentration and charge ratio. The gel also shows the DNA digestion by DNase with or without the presence of dendrimers. The presence of dendrimer reduces the DNA progression and protects the DNA from DNase digestion.

3. Gel Electrophoresis

By gel electrophoresis it was possible to follow the DNA compaction caused by the presence of dendrimers, Figure 5. It can be observed that the intensity of the smeared band corresponding to free salmon sperm DNA decreases for higher amounts of dendrimers in the DNA solutions. At the same time, the intensity in the wells increases which indicates the presence of complexes unable to be transported through the gel. This result shows that the dendrimers are very efficient in the condensation of DNA. It should be noted that there exist two possible explanations to the DNA detected in the gel wells. One is that the reduction of negative charges of the DNA molecules, when it is complexed by dendrimers, will reduce the DNA progression caused by the electric field through the gel. The other is the fact that the size of some of the DNA containing aggregates could be too big to be able to enter the gel pores.

The relation between DNA digestion and the presence of dendrimers was also studied by incubating the samples with Turbo DNase. Turbo DNase is efficient at degrading DNA when freely accessible. When dendrimers are present, the complexes formed act to protect DNA from degradation since the DNA accessibility to the DNase is reduced. The results are presented in Figure 5 where it is possible to view the increased retardation of the DNA in the presence of increased amount of dendrimers, for a few of the ratios investigated. It should be noted that the salmon sperm DNA band appearing on agarose gels is smeared since the DNA is not totally monodisperse but rather containing

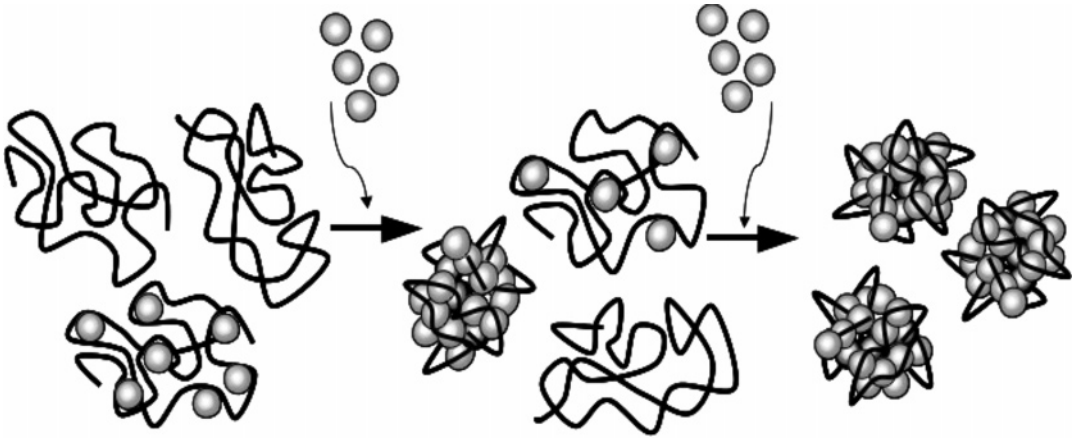

Figure 6. Proposed binding model for discrete aggregates formed between DNA and PAMAM dendrimers of generation 4. A coexistence of coils and globules are shown for low ratios of dendrimers/DNA ($r_{molar} < 30$), and only compacted globules are displayed for higher amounts of dendrimers in dilute solutions below charge neutrality.

2000 ± 500 bp as stated by the manufacturer. Gel electrophoresis performed on a more monodisperse DNA sample (linearized T7DNA, 4331 bp) present less smeared bands. The results show similar trends and are in agreement with those presented here.[33] It is also seen that the band corresponding to free salmon sperm DNA disappears in all samples treated with DNAse. For the control sample with free DNA, no visible DNA bands can be detected in the presence of 0.5 μL (2 units) of Turbo DNase when incubated for 5 min and more. For the ratio of 10 dendrimers and higher, some fluorescence was detected in the wells meaning that the DNA totally complexed in the form of neutral or precipitated aggregates is protected to the action of the enzyme, at least for the time period investigated. A weak intensity in the form of a smeared band at a slightly lower molecular weight is also detected for the dendrimer containing samples indicating that DNA digestion was taking place, but the kinetics is slower in the presence of dendrimers. When incubating the gel samples with Turbo DNase for 60 min or longer, DNA is degraded although dendrimers of all the different dendrimer/DNA ratios investigated are present in the samples. This concludes that the aggregate structure is relatively open, allowing the enzyme to catalyze DNA digestion on the exterior of the dendrimer/DNA aggregate. This process will lead to complete digestion with time.

Conclusions

The binding interaction between salmon sperm DNA of 2000 bp and PAMAM dendrimers of generation four has been investigated. Results based on DLS and steady-state fluorescence spectroscopy as well as gel electrophoresis has made it possible to propose a binding model, which is presented in Figure 6. Experimental results shown here are in agreement with Monte Carlo simulation studies where a packing model for semiflexible chains and macroions were studied.[34−36] If the DNA as being a semiflexible chain with a contour length of 680 nm is thought to wrap one turn around each dendrimer having a circumference of 14 nm, a maximum of 49 dendrimers could be interacting with one DNA molecule. Taking the same percentage of linker DNA into account as when DNA is condensed into nucleosomes gives a resulting number of 35 dendrimers for each DNA molecule.[37] This calculation is in good agreement with the fluorescence spectroscopy results shown. The results also agree with the study of DNA digestion using DNase performed with gel electrophoresis. The fact that dendrimers reduce the rate of DNA degradation but are unable to completely protect the DNA is in agreement with the open aggregate structure proposed. DNase is suggested to initiate digestion by acting on the loops or linker pieces of DNA protruding into the solution. With enough time, all DNA will be accessible to the DNase. The variation in the hydrodynamic radius of the aggregate measured with DLS for the different ratios could also be explained by a flexible aggregate structure.

The difference between the DLS and fluorescence spectroscopy results in terms of the amount of dendrimers in one aggregate can be explained by the higher concentration used in the DLS measurements. The probability for dendrimers to aggregate with each other would be higher and more dendrimers will then be required to condense all DNA into discrete aggregates. It is concluded in this study that it is possible to form discrete aggregates composed of one DNA molecule and roughly 35 dendrimers in dilute solutions. The complex formation process was found to be cooperative, as pictured in Figure 6 showing the coexistence of both condensed DNA and free DNA in its native form.

The polydispersity of the salmon sperm DNA is thought not to affect the conclusions made from the results presented here. Fluorescence spectroscopy as well as gel electrophoresis data (already stated) using monodisperse linearized T7DNA (4331 bp), are in good agreement with results published here.[33]

Future studies will focus on further relating the aggregate size and the complex formation process to the DNA used as well as the relation between aggregate structure and ability to transcribe and translate the genetic material.

Acknowledgment. The sixth EU framework program is greatly acknowledged for funding this work as being a part of a EU-STREP project with NEST program (NEONUCLEI, Contract 12967).

References and Notes

(1) Hayakawa, K.; Santerre, J. P.; Kwak, J. C. T. *Biophys. Chem*. **1983**, *17*, 175−181.
(2) Shirashama, K.; Takashima, K.; Takisawa, N. *Bull. Chem. Soc. Jpn.* **1987**, *60*, 43−47.
(3) Bhattacharya, S.; Mandal, S. S.; *Biochim. Biophys. Acta* **1997**, *1323*, 29−44.
(4) Kikuchi, I. S.; Carmona-Ribeiro, A. M. *J. Phys. Chem. B* **2000**, *104*, 2829−2835.
(5) Wagner, K.; Harries, D.; May, S.; Kahl, V.; Rädler, J. O.; Ben-Shaul, A. *Langmuir* **2000**, *16*, 303−306.
(6) Lasic, D. D. *Liposomes in Gene Delivery*; CRCPress: Boca Raton, FL, 1997.

(7) Pötschke, D.; Ballauff, M.; Lindner, P.; Fischer, M.; Vögtle, F. *Macromol. Chem. Phys.* **2000**, *201*, 330−339.
(8) Rosenfeldt, S.; Dingenouts, N.; Ballauff, M.; Lindner, P.; Likos, C. N.; Werner, N.; Vögtle, F. *Macromol. Chem. Phys.* **2002**, *203*, 1995−2004.
(9) Likos, C. N.; Rosenfeldt, S.; Dingenouts, N.; Balluff, M.; Werner, N.; Vögtle, F. *J. Chem. Phys.* **2002**, *117*, 1869−1877.
(10) Bayele, H. K.; Sakthivel, T.; O'Donnel, M.; Pasi, K. J.; Wilderspin, A. F.; Lee, C. A.; Toth, I.; Florence, A. T. *J. Pharm. Sci.* **2005**, *94*, 446−457.
(11) Bielinska, A. U.; Kukowska-Latallo, J. F.; Baker, J. R., Jr. *Biochim. Biophys. Acta* **1997**, *1353*, 180−190.
(12) Mitra, A; Imae, T. *Biomacromol.* **2004**, *5*, 69−73.
(13) Tang, M. X.; Szoka, F. C. *Gene Ther.* **1997**, 823−832.
(14) Ottaviani, F.; Furini, F.; Casini, A.; Turro, N.; Jockusch, S.; Tomalia, D. A.; Messori, L. *Macromolecules* **2000**, *33*, 7842−7851.
(15) Eichman, J. D.; Bielinska A. U.; Kukowska-Latallo, J. F.; Baker, J. R., Jr. *Pharm. Sci. Technol. Today* **2000**, *3*, 232−245.
(16) Svenson S.; Tomalia, D. A. *Adv. Drug Delivery Rev.* **2005**, *57*, 2106−2129.
(17) Hellweg, T.; Henry-Toulmé, N.; Chambon, M.; Roux, D. *Colloid Surf. A* **2000**, *163*, 71−80.
(18) Milhem, O. M.; Myles, C.; McKeown, N. B.; Attwood, D.; D'Emanuele, A. *Int. J. Pharm.* **2000**, *197*, 239−241
(19) El-Sayed, M.; Kiani, M. F.; Naimark, M. D.; Hikal, A. H.; Ghandehari, H. *Pharm. Res.* **2001**, *18*, 23−28
(20) Cakara, D.; Kleimann, J.; Borkovec, M. *Macromolecules* **2003**, *36*, 4201−4207.
(21) Jansson, J.; Schillén, K.; Olofsson, G.; Cardoso da Silva, R.; Loh, W. *J. Phys. Chem. B* **2004**, *108*, 82−92.
(22) Jockusch, S.; Turro, N. J.; Ottaviani, M. F.; Tomalia, D. A. *J. Colloid Interface Sci.* **2002**, *256*, 223−227.
(23) Sorlie, S. S.; Pecora, R. *Macromolecules* **1988**, *21*, 1437−1449.
(24) Sorlie, S. S; Pecora, R. *Macromolecules* **1990**, *23*, 487−497.
(25) Cárdenas, M.; Dreiss, C. A.; Nylander, T.; Chan, C.; Cosgrove, T.; Lindman, B. *Langmuir* **2005**, *21*, 3578−3583.
(26) Cárdenas, M.; Schillén, K.; Nylander, T.; Jansson, J.; Lindman, B. *Phys. Chem. Chem. Phys.* **2004**, *6*, 1603−1607.
(27) Chen, W.; Turro, N. J.; Tomalia, D. A. *Langmuir* **2000**, *16*, 15−19.
(28) Dias, R. S.; Lindman, B.; Miguel, M. G. *J. Phys. Chem. B* **2002**, *106*, 12608−12612.
(29) Dias, R. S.; Pais, A. A. C. C.; Miguel, M. G.; Lindman. B. *Colloid Surf. A* **2004**, *250*, 115−131.
(30) Mel'nikov, S. M.; Sergeyev, V. G.; Yoshikawa, K. *J. Am. Chem. Soc.* **1995**, *117*, 2401−2408.
(31) Mel'nikova, Y. S.; Mel'nikov, S. M.; Löfroth, J.-E. *Biophys. Chem.* **1999**, *81*, 125−141.
(32) Eastman, S. J.; Siegel, C.; Tousignant, J.; Smith, A. E.; Cheng, S. H.; Scheule, R. K. *Biochim. Biophys. Acta* **1997**, *1325*, 41−62.
(33) Örberg, M.-L.; Dias, R. S.; Muck, J.; Zink, D.; Nylander, T. Manuscript in preparation.
(34) Jonsson, M.; Linse, P. *J. Chem. Phys.* **2001**, *115*, 3406−3418.
(35) Jonsson, M.; Linse, P. *J. Chem. Phys.* **2001**, *115*, 10975−10985.
(36) Akinchina, A.; Linse, P. *J. Phys. Chem. B* **2003**, *107*, 8011−8021.
(37) Stryer, L.; *Biochemistry*, 4th ed.; W. H. Freeman and Company: New York, 1995; pp 975−1008.

BM061194Z